

# Influence of Surface Diffusion on the Formation of Hollow Nanostructures Induced by the Kirkendall Effect: The Basic Concept

Hong Jin Fan,<sup>\*,†,‡</sup> Mato Knez,<sup>†</sup> Roland Scholz,<sup>†</sup> Dietrich Hesse,<sup>†</sup>  
Kornelius Nielsch,<sup>†</sup> Margit Zacharias,<sup>†,§</sup> and Ulrich Gösele<sup>†</sup>

*Max Planck Institute of Microstructure Physics, Weinberg 2, 06120 Halle, Germany,  
Department of Earth Sciences, University of Cambridge, Cambridge CB2 3EQ,  
United Kingdom, Department of Physics, University of Paderborn,  
Warburger Strasse 100, 33098 Paderborn, Germany*

Received January 4, 2007; Revised Manuscript Received March 1, 2007

## ABSTRACT

The Kirkendall effect has been widely applied for fabrication of nanoscale hollow structures, which involves an unbalanced counterdiffusion through a reaction interface. Conventional treatment of this process only considers the bulk diffusion of growth species and vacancies. In this letter, a conceptual extension is proposed: the development of the hollow interior undergoes two main stages. The initial stage is the generation of small Kirkendall voids intersecting the compound interface via a bulk diffusion process; the second stage is dominated by surface diffusion of the core material (viz., the fast-diffusing species) along the pore surface. This concept applies to spherical as well as cylindrical nanometer and microscale structures, and even to macroscopic bilayers. As supporting evidence, we show the results of a spinel-forming solid-state reaction of core–shell nanowires, as well as of a planar bilayer of ZnO–Al<sub>2</sub>O<sub>3</sub> to illustrate the influence of surface diffusion on the morphology evolution.

The Kirkendall effect is a classical phenomenon in metallurgy.<sup>1–3</sup> It basically refers to a nonequilibrium mutual diffusion process through an interface of two metals so that vacancy diffusion occurs to compensate for the unequal material flow. In planar metallic bilayers, this effect can give rise to void formation near the bond interface and within the fast-diffusion side,<sup>4–6</sup> thus deteriorating the bonding strength of the interface. In a spherical material system where the fast-diffusion phase is enclosed by the slower one, the Kirkendall effect can also apply and manifest itself by forming hollow crystals composed of a compound shell. This concept was first demonstrated by Aldinger,<sup>7</sup> who obtained shells of a BeNi alloy after annealing Ni-coated Be micro-particles (of 33  $\mu\text{m}$  diameter). Coming to the nanoscale, due to the structural perfection and wide availability of single-crystal metal nanoparticles, the Kirkendall effect can result in smooth and uniform-sized hollow compound nanocrystals. This was first demonstrated by the group of Alivisatos for spherical hollow nanocrystals<sup>8</sup> and later on by various other groups.<sup>9–11</sup> An extension to cylindrical nanotubes,<sup>12–14</sup> has

recently been reported via either a solid–solution, solid–gas, or solid–solid reaction. Although not specified, such an effect might have also been the driving force for formation of some other hollow nanocrystals, e.g., gold<sup>15</sup> and AuPt bimetallic<sup>16</sup> nanoshells synthesized in solution. It is believed that the use of the Kirkendall effect allows a rational design of nanoscale hollow objects, from metals, semiconductors to insulators, based on the proper choice of materials and different reaction properties known from thin-film diffusion couples.

In the study of kinetics of the Kirkendall-type diffusion, the conventional model employs a one-dimensional steady-state bulk flux governed by Fick's first law (i.e., diffusion driven by concentration gradient). For spherical nanostructures, Tu and Gösele<sup>17</sup> considered the Gibbs–Thomson effect in the thickening rate of the compound layer (i.e., diffusion driven by decrease in surface free energy due to curvature difference) and studied the thermal stability of a hollow nanocrystal. In their follow-up work, Yin et al.<sup>18</sup> dealt with the kinetics of the volume flux and derived the empirical criteria and time scale for the formation of hollow nanostructures. In all these treatments, the void growth rate is determined merely by the inward flux of vacancies, which

\* Corresponding author. E-mail: hjfan@mpi-halle.de.

<sup>†</sup> Max Planck Institute of Microstructure Physics.

<sup>‡</sup> University of Cambridge.

<sup>§</sup> University of Paderborn.

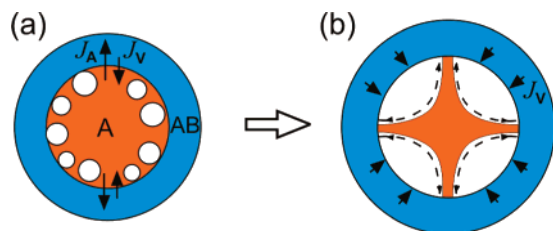


**Figure 1.** Generalized model for hollow structure formation based on a “Kirkendall effect + surface diffusion” process (see text for details).

exclusively depends on the concentration gradients of both phases,  $\nabla C_i$ , across the compound shell and the difference in their bulk diffusivity  $D_i^B$ .

On the other hand, pores could also grow via surface diffusion<sup>19</sup> on an existing or early established channel. In fact, surface diffusion is an important mass transport mechanism in powder sintering of metals and ceramics, which gives rise to coarsening and enhancement of pore growth.<sup>20–26</sup> Furthermore, it has been recognized that surface diffusion can be the main mechanism accounting for the elongation of carbon nanotubes,<sup>27,28</sup> and inorganic nanowire/tubes,<sup>29,30</sup> when the characteristic diffusion length  $(D_s \tau_s)^{1/2} > l$  (length of a nanowire or tube). In the study of carbonization of a crystalline Si substrate, Scholz et al.<sup>31</sup> observed micropipes extending inward from the Si surface. According to the authors, a self-adjusting process was involved in which Si out-diffuses over the wall of the pipes to the wafer surface, where Si finally reacts to form SiC. Even in the extreme Kirkendall process for Be–Ni spherical particles,<sup>7</sup> the self-diffusion of Be atoms along the skeletal surface is a most likely route for mass transport to the BeNi shell.

In this letter, we propose a conceptual extension for the growth process of voids in Kirkendall-diffusion systems, particularly in nanoscale materials, which involves surface diffusion via the pore surfaces as an essential transport path. To support our hypothesis, we will show experimental evidence using the  $\text{ZnAl}_2\text{O}_4$  spinel-forming reaction as a model and discuss the influence of surface diffusion on the structural evolution.

In a nanoscale system, due to the finite volume and spatial confinement, a high vacancy supersaturation can readily be reached so that void formation is enhanced compared to the bulk counterparts. In this light, the voids have a high chance to touch the compound outer layer. Figure 1 shows schematically our generalized model. For the diffusion flux, we assume  $J_A > J_B$ . In the initial stage (Figure 1a), Kirkendall voids are generated near the A/AB interface during vacancy-assisted exchange of material via bulk interdiffusion. The voids are the sinks for subsequent inward flux of vacancies ( $J_V = J_A - J_B$ ) and thus grow in size. The voids coalesce into bigger ones and touch the compound layer AB, in one sense breaking the connection for lattice diffusion and in the other sense establishing new bridges as fast transport paths for the remaining material A (Figure 1b). At this stage, diffusion of adatoms of the remaining material A along the bridges, i.e., the pore surface, to the reaction front becomes the dominant material transport process because of a much

lower activation energy ( $Q$ ) and higher diffusion coefficient of surface diffusion (index “S”) than those of bulk diffusion (index “B”). For example, for ZnO,  $Q_S = 158$  kJ/mol,<sup>32</sup> while  $Q_B = 347–405$  kJ/mol;<sup>33</sup> for  $\text{TiO}_2$  (at 800 °C),  $D_S = 6.5 \times 10^{-14}$  (cm<sup>2</sup>/s),  $D_B = 3.5 \times 10^{-16}$  (cm<sup>2</sup>/s).<sup>23</sup> The A material can redistribute itself at the open surface of the AB layer via fast surface diffusion. Within the AB shell, the material exchange mechanism remains the same, viz, bulk interdiffusion associated with Kirkendall effect. Therefore vacancies are continuously generated and flow inward.

Such bridges have been observed in the intermediate reaction stage of colloidal cobalt sulfide sub-20 nm nanocrystals,<sup>8</sup> and in the 160–500 nm diameter CdS hemispheres by solid–vapor reaction,<sup>12</sup> as well as the 33  $\mu\text{m}$  sized BeNi alloy cages after complete solid–solid alloy formation.<sup>7</sup> Kirkendall-type diffusion occurs in all these experiments. In particular, a time-sequenced reaction in ref 8 revealed evidently the evolution of a bridge structure. For ZnO itself, zinc diffuses roughly 2 orders of magnitude faster than oxygen in single-crystal ZnO.<sup>34</sup> Our previous report on formation of hollow ZnO cages through an in situ oxidation of micron sized (3–5  $\mu\text{m}$ ) Zn particles,<sup>35</sup> as well as those subsequently reported by similar methods,<sup>36–38</sup> might also be examples of Kirkendall voids combined with strong transport by surface diffusion, especially when cracks are present in the shell.

Here we provide more explicit evidence using  $\text{ZnAl}_2\text{O}_4$  as a model system, where hollow spinel  $\text{ZnAl}_2\text{O}_4$  nanowires were formed through a solid–solid reaction of  $\text{ZnO}–\text{Al}_2\text{O}_3$  core–shell nanowires. Details of the fabrication were published elsewhere.<sup>13</sup> The reaction has been established as an effectively one-way transfer of ZnO into alumina<sup>39,40</sup> and therefore represents a case of an extreme Kirkendall effect. In this report, the ZnO nanowires have diameters in the range of 10–60 nm, while the thickness of the  $\text{Al}_2\text{O}_3$  shell was fixed around 10 nm. Conformal coating of the alumina layer was realized by atomic layer deposition at 200 °C using  $[\text{Al}(\text{CH}_3)_3]$  and water as the aluminum and oxygen source, respectively.<sup>13,41</sup> Such formed  $\text{ZnO}–\text{Al}_2\text{O}_3$  core–shell nanowires were then annealed in an open tube furnace at 700 °C for 3 h.

Figure 2 shows the transmission electron microscopy (TEM) images of structures after annealing under identical conditions. Complete hollow spinel nanotubes were formed, as seen in Figure 2a, when the thickness of the initial ZnO nanowires is close to 10 nm. In Figure 2b–d, all the ZnO nanowires are thicker than necessary (10–15 nm) for a complete reaction with the 10 nm thick alumina shell. The morphology details of the remaining ZnO core can represent intermediate states of a hypothetical thorough reaction with a thicker  $\text{Al}_2\text{O}_3$  layer. In Figure 2b, where the initial ZnO nanowire thickness is in the range of 19–21 nm, interrupted tubes with segmented voids sandwiched by the remaining ZnO are shown. This is because of the preferential enlargement of some early established voids by losing surface atoms. In Figure 2c, where the initial ZnO nanowires are 32–37 nm thick, the main feature (especially in the off-tip parts) is a cellular ZnO remainder. Big voids are observed in contact

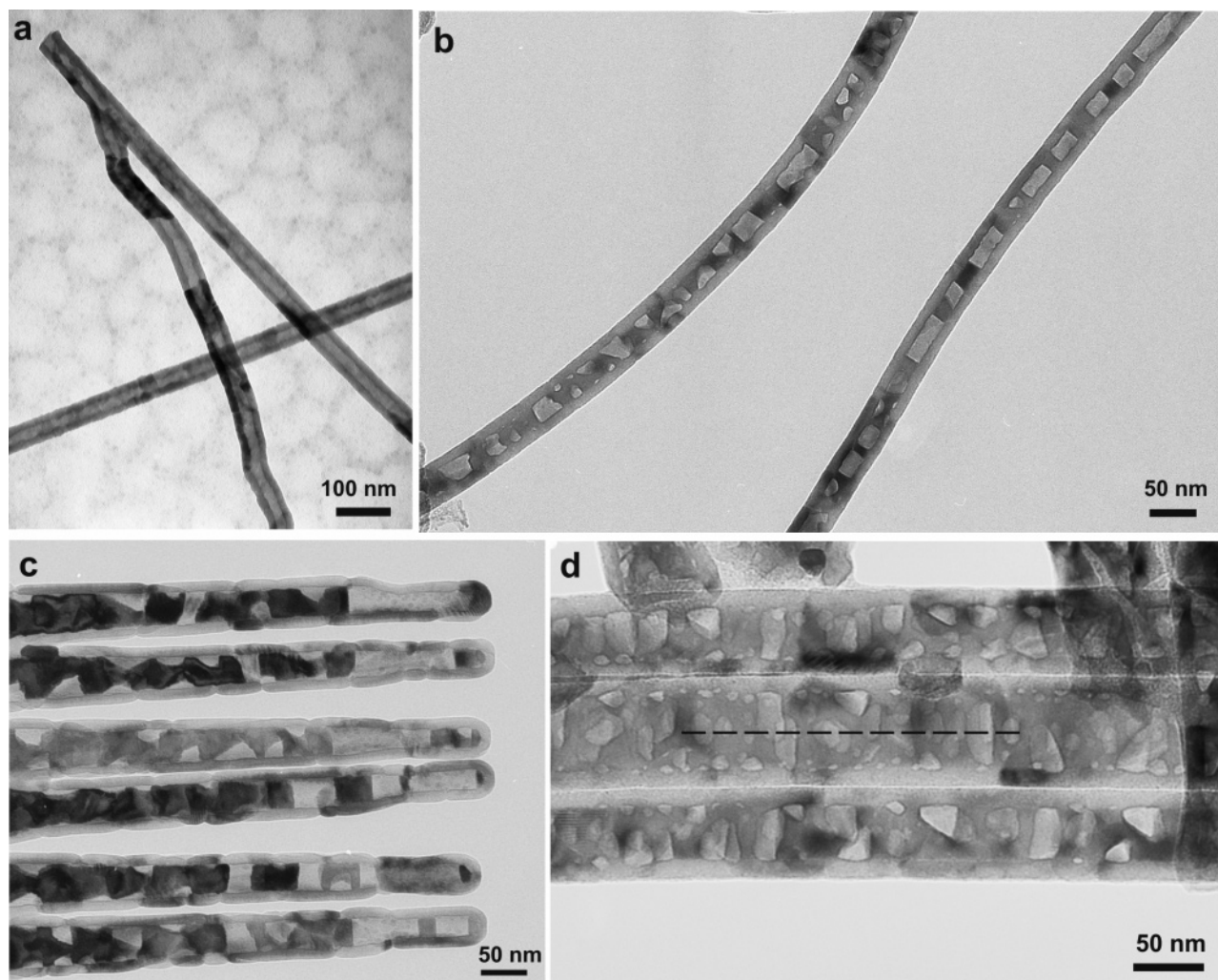


**Figure 2.** TEM images of structure formed after a  $\text{ZnAl}_2\text{O}_4$  spinel-forming reaction on the ZnO nanowire surface. The diameters of the initial ZnO nanowires are  $\approx 10$  nm in (a), 19–21 nm in (b), 32–37 nm in (c), and 39–51 nm in (d). The conditions for atomic layer deposition of  $\text{Al}_2\text{O}_3$  are identical and the  $\text{Al}_2\text{O}_3$  thickness is about  $\approx 10$  nm in all cases shown. The dashed line is a guide for the eye to see the void size variance.

with the spinel shell. In Figure 2d, the thicknesses of ZnO nanowires, 39–51 nm, are even larger than necessary. After reaction, characteristic voids are seen mostly in the proximity of the spinel shell, similar to a planar interface, as we will see below. Some voids are significantly large, e.g., see along the dashed line in Figure 2d. If the reaction were a pure bulk diffusion-controlled process, it is expected that a chain of Kirkendall voids of similar size existed near the inner surface. Hence, Figure 2d implies the occurrence of a “Kirkendall  $\rightarrow$  surface diffusion” process as proposed above.

Surface diffusion can be enhanced by specific conditions, for example, higher annealing temperatures (e.g., MgO and  $\text{Al}_2\text{O}_3$ <sup>22</sup>), higher gas pressure (e.g.,  $\text{TiO}_2$ <sup>23</sup>), and ambient type (e.g.,  $\text{RuO}_2$  and  $\text{Pt}$ <sup>42,43</sup>). On one hand, the surface diffusion process should accelerate the reaction and thus reduce the time for the formation of a complete single hole inside the AB shell. On the other hand, it enhances the local growth of voids and results in structural irregularities like a skeletal interior. As a consequence, an intentional fabrication of complete hollow nanocrystals or nanotubes using the Kirkendall effect becomes more complex. This is a problem

especially for core–shell nanowires when the inner core exceeds the available shell material: the uneven flux of inner constituent in the cylindrical coordination easily gives rise to segmented tubes, as exemplified by Figure 2b. Nevertheless, one might still eventually obtain complete nanotubes by further etching away or dissolving the remaining skeletal core, for example, dissolving ZnO in diluted HCl acid.

Our model also applies to the growth of Kirkendall voids at a bilayer planar interface. Figure 3 shows the result from an experiment (same conditions for  $\text{Al}_2\text{O}_3$  deposition and annealing as above) on a sufficiently thick ZnO film. A string of voids are clearly seen at the interface and mainly within the ZnO surface layer, characteristic of Kirkendall-type diffusion. Some of the voids are much larger than the rest, which is most likely because of a locally enhanced growth accompanied by surface diffusion of ZnO rather than coarsening. A closer view of one of the big voids, as well as the crystalline spinel film, is given in Figure 3c. This provides strong evidence that the void was formed during the reactive annealing process, rather than being an initial surface defect of the ZnO, which would otherwise have a



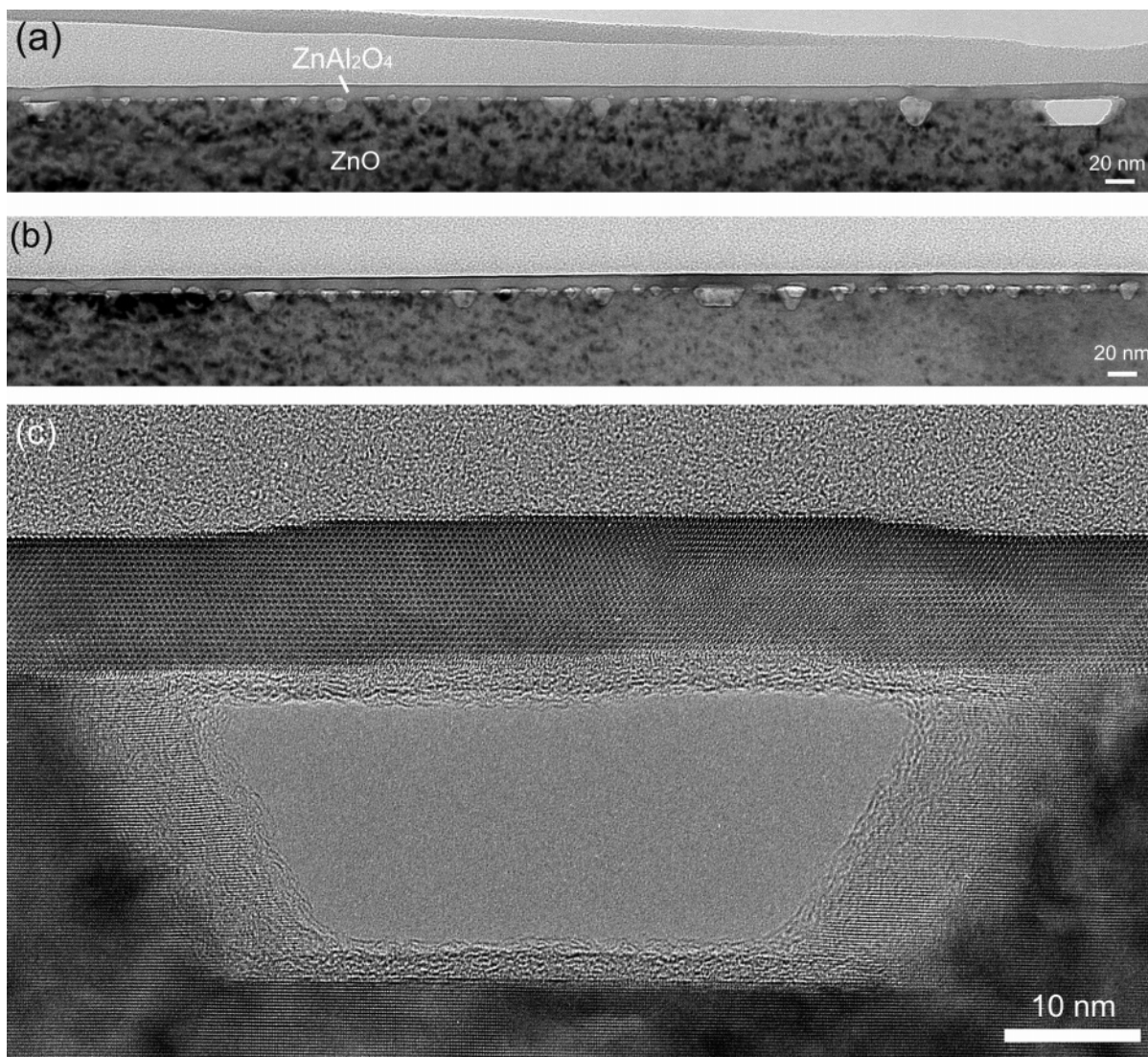


**Figure 3.** Kirkendall voids at a ZnO–Al<sub>2</sub>O<sub>3</sub> planar interface. (a,b) Cross-section TEM image of the interface area after annealing, showing a distribution of random-sized Kirkendall voids. (c) Close-up view of one big void and the single-crystal top spinel layer.

uniform covering of the spinel layer along the step edges. It is noteworthy that the spinel layer above this big void is 3 atomic layers higher than its surroundings. This could be a result of enhanced reaction above the void. It is worth mentioning that the void size distribution as well as the shape in Figure 3 is qualitatively the same as those examined by Radi, Barna, and Labar<sup>5</sup> in their study of solid–vapor Al–Pt reaction. This corroborates the mechanism that Al atoms migrate to the free surface area of the alloy layer bordering the Kirkendall voids via diffusion on the void surface.

In conclusion, a conceptual extension for the formation of hollow nanostructures initiated by the Kirkendall effect is proposed, suggesting that surface diffusion processes might be the dominant mass flow mechanism responsible for the enlargement of the interior pores after their initial nucleation and formation induced by the Kirkendall effect. We showed results of the spinel-forming solid-state reaction of ZnO–Al<sub>2</sub>O<sub>3</sub> core–shell nanowires as supporting evidence to illustrate the influence of surface diffusion on the morphology evolution. With this concept, we expect that the formation

of complete hollow structures, as experimentally demonstrated in several publications, is faster than that computed by considering only bulk diffusion. Furthermore, we believe that the “Kirkendall effect + surface diffusion” mechanism should also apply to macroscopic core–shell structures as well as to planar bilayers.

## References

- (1) For an introductory view, see: Nakajima, H. *J. Miner. Met. Mater. Soc.* **1997**, *49*, 15.
- (2) Smigelskas, A. D.; Kirkendall, E. O. *Trans. AIME* **1947**, *171*, 130.
- (3) Paul, A. Ph.D. Thesis. Technische Universiteit Eindhoven, The Netherlands, 2004.
- (4) Schröder, H.; Samwer, K.; Köster, U. *Phys. Rev. Lett.* **1985**, *54*, 197.
- (5) Radi, Zs.; Barna, P. B.; Labar, J. *J. Appl. Phys.* **1996**, *79*, 4096.
- (6) Zeng, K.; Stierman, R.; Chiu, T.-C.; Edwards, D.; Ano, K.; Tu, K. *N. J. Appl. Phys.* **2005**, *97*, 024508.
- (7) Aldinger, F. *Acta Metall.* **1974**, *22*, 923.
- (8) Yin, Y.; Rioux, R. M.; Erdonmez, C. K.; Hughes, S.; Somorjai, G. A.; Alivisatos, A. P. *Science* **2004**, *304*, 711.
- (9) Wang, Y.; Cai, L.; Xia, Y. *Adv. Mater.* **2005**, *17*, 473.
- (10) Wang, C. M.; Baer, D. R.; Thomas, L. E.; Amonette, J. E.; Antony, J.; Qiang, Y.; Duscher, G. *J. Appl. Phys.* **2005**, *98*, 094308.

- (11) Gao, J.; Zhang, B.; Zhang, X.; Xu, B. *Angew. Chem., Int. Ed.* **2006**, *45*, 1220.
- (12) Li, Q.; Penner, R. M. *Nano Lett.* **2005**, *5*, 1720.
- (13) Fan, H. J.; Knez, M.; Scholz, R.; Nielsch; Pippel, E.; Hesse, D.; Zacharias, M.; Gösele, U. *Nat. Mater.* **2006**, *5*, 627.
- (14) Ng, C. H. B.; Tan, H.; Fan, W. Y. *Langmuir* **2006**, *22*, 9712.
- (15) Sun, Y.; Xia, Y. *Science* **2002**, *298*, 2176.
- (16) Liang, H. P.; Guo, Y. G.; Zhang, H. M.; Hu, J. S.; Wan, L. J.; Bai, C. L. *Chem. Commun.* **2004**, 1496.
- (17) Tu, K. N.; Gösele, U. *Appl. Phys. Lett.* **2005**, *86*, 093111.
- (18) Yin, Y.; Erdonmez, C. K.; Cabot, A.; Hughes, S.; Alivisatos, A. P. *Adv. Funct. Mater.* **2006**, *16*, 1389.
- (19) Burton, W. K.; Cabrera, N.; Frank, F. C. *Philos. Trans. R. Soc. London, Ser. A.* **1951**, *243*, 299.
- (20) Kuczynski, G. C. *Trans. AIME* **1949**, *185*, 169.
- (21) Whittemore, O. J.; Varela, J. A. *J. Am. Ceram. Soc.* **1981**, *64*, C154.
- (22) Sajgalik, P.; Panek, Z.; Uhrik, M. *J. Mater. Sci.* **1987**, *22*, 4460.
- (23) Nanko, M.; Ishizaki, K. *Phys. Rev. B.* **1997**, *56*, 6965.
- (24) Akash, A.; Mayo, M. J. *J. Am. Ceram. Soc.* **1999**, *82*, 2948.
- (25) Shi, J. L.; Deguchi, Y.; Sakabe, Y. *J. Mater. Sci.* **2005**, *40*, 5711.
- (26) Han, J. P.; Mantas, P. Q.; Senos, A. M. R. *J. Am. Ceram. Soc.* **2005**, *88*, 1773.
- (27) Louchev, O. A.; Laude, T.; Sato, Y.; Kanda, H. *J. Chem. Phys.* **2003**, *118*, 7622.
- (28) Louchev, O. A.; Kanda, H.; Rosén, A.; Bolton, K. *J. Chem. Phys.* **2004**, *121*, 446.
- (29) Louchev, O. A. *Appl. Phys. Lett.* **1997**, *71*, 3522.
- (30) Schubert, L.; Werner, P.; Zakharov, N. D.; Gerth, G.; Kolb, F. M.; Long, L.; Gösele, U.; Tan, T. Y. *Appl. Phys. Lett.* **2004**, *84*, 4968.
- (31) Scholz, R.; Gösele, U.; Niemann, E.; Leidich, D. *Appl. Phys. Lett.* **1995**, *67*, 1453.
- (32) Birnboim, A.; Olorunyolemi, T.; Carmel, Y. *J. Am. Ceram. Soc.* **2001**, *84*, 131.
- (33) Tomlins, G. W.; Routbort, J. L.; Mason, T. O. *J. Am. Ceram. Soc.* **1998**, *81*, 869.
- (34) Hynes, A. P.; Doremus, R. H.; Siegel, R. W. *J. Am. Ceram. Soc.* **2002**, *85*, 1979.
- (35) Fan, H. J.; Scholz, R.; Kolb, F. M.; Zacharias, M.; Gösele, U. *Solid State Commun.* **2004**, *130*, 517.
- (36) Xia, X. H.; Zhu, L. P.; Ye, Z. Z.; Yuan, G. D.; Zhao, B. H.; Qian, Q. *J. Cryst. Growth* **2005**, *282*, 506.
- (37) Ravindran, S.; SenthilAndavan, G. T.; Ozkan, C. *Nanotechnology* **2006**, *17*, 723.
- (38) Sulieman, K. M.; Huang, X. T.; Liu, J. P.; Tang, M. *Nanotechnology* **2006**, *17*, 4950.
- (39) Branson, D. L. *J. Am. Ceram. Soc.* **1965**, *48*, 591.
- (40) Keller, J. T.; Agrawal, D. K.; McKinstry, A. *Adv. Ceram. Mater.* **1988**, *3*, 420.
- (41) Fan, H. J.; Knez, M.; Scholz, R.; Nielsch, K.; Pippel, E.; Hesse, D.; Gösele, U.; Zacharias, M. *Nanotechnology* **2006**, *17*, 5157.
- (42) Horch, S.; Lorensen, H. T.; Helveg, S.; Lægsgaard, E.; Stensgaard, I.; Jacobsen, K. W.; Nørskov, J. K.; Besenbacher, F. *Nature* **1998**, *398*, 134.
- (43) Kim, J. D.; Kang, B. S.; Noh, T. W.; Yoon, J. G.; Baik, S. I.; Kim, Y. W. *J. Electrochem. Soc.* **2005**, *152*, D23.

NL070026P